Accepted Manuscript

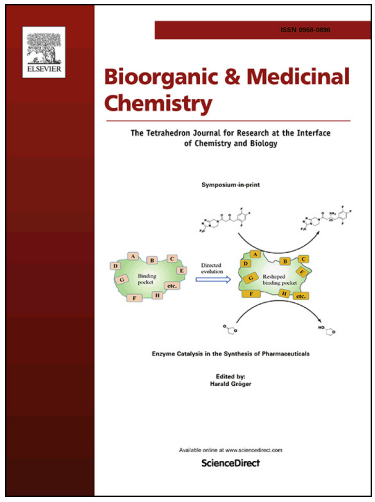

Novel amino acid-substituted diphenylpyrimidine derivatives as potent BTK inhibitors against B cell lymphoma cell lines

Changyuan Wang, Si Li, Qiang Meng, Xiuli Sun, Hua Li, Xiaohong Shu, Huijun Sun, Kexin Liu, Zhihao Liu, Xiaodong Ma

PII: S0968-0896(18)30826-5
DOI: https://doi.org/10.1016/j.bmc.2018.07.007
Reference: BMC 14444

To appear in: *Bioorganic & Medicinal Chemistry*

Received Date: 27 April 2018
Revised Date: 15 June 2018
Accepted Date: 5 July 2018

Please cite this article as: Wang, C., Li, S., Meng, Q., Sun, X., Li, H., Shu, X., Sun, H., Liu, K., Liu, Z., Ma, X., Novel amino acid-substituted diphenylpyrimidine derivatives as potent BTK inhibitors against B cell lymphoma cell lines, *Bioorganic & Medicinal Chemistry* (2018), doi: https://doi.org/10.1016/j.bmc.2018.07.007

Novel amino acid-substituted diphenylpyrimidine derivatives as potent BTK inhibitors against B cell lymphoma cell lines

Changyuan Wang [a,1], Si Li [a,1], Qiang Meng [a], Xiuli Sun [c], Hua Li [a], Xiaohong Shu [a], Huijun Sun [a], Kexin Liu [a], Zhihao Liu [a,b *] and Xiaodong Ma [a, *]

[a] *College of Pharmacy, College of laboratory medicine, Dalian Medical University, Dalian 116044, PR China*

[b] *State Key Laboratory of Bioactive Substance and Function of Natural Medicines, Institute of Materia Medica, Chinese Academy of Medical Sciences and Peking Union Medical College, Beijing 100050, P. R. China*

[c] *Department of Hematology, the First Affiliated Hospital of Dalian Medical University, Dalian 116011, PR China*

[1] *These authors contributed equally to this work*

[*] *Corresponding author*

E-mail address: *xiaodong.ma@139.com (X. Ma), liuzhihao12399@126.com (Z. Liu)*

Abstract

A new family of diphenylpyrimidine derivatives bearing an amino acid substituent were identified as potent BTK inhibitors. Among them, compound **7b**, which features an L-proline substituent, was identified as the strongest BTK inhibitor, with an IC_{50} of 8.7 nM. Compound **7b** also displayed similar activity against B-cell lymphoma cell lines as ibrutinib. Moreover, **7b** exhibited low cytotoxic activity against normal PBMC cells. In addition, the acridine orange/ethidium bromide (AO/EB) staining assay, Western blot analysis and flow cytometry analysis also showed its effectiveness in interfering with B-cell lymphoma cell growth. The molecular simulation performance showed that **7b** forms additional strong hydrogen bonds with the BTK protein. All these findings provided new clues about the pyrimidine scaffold as an effective BTK inhibitor for the treatment of B-cell lymphoma.

1. Introduction

Bruton's tyrosine kinase (BTK), a member of the Tec family of non-receptor tyrosine kinases, plays a key role in the B-cell signaling pathway linking the cell surface B-cell receptor (BCR) stimulation to downstream intracellular responses [1-3]. A number of B-cell-derived malignancies, including chronic lymphocytic leukemia (CLL), acute lymphoblastic leukemia (ALL), mantle cell lymphoma (MCL), Waldenström's macroglobulinemia (WM) and multiple myeloma (MM), are related to the dysregulation of BTK kinase [4,5]. Ibrutinib is the first-in-class BTK inhibitor, which demonstrated high efficacy in patients with CLL, MCL, WM, MM, *etc*. [6-8]. Additionally, a number of covalent and noncovalent BTK inhibitors, including spebrutinib (**2**) (ClinicalTrials.gov identifier: NCT01744626) [9], and PLS-123 (**3**) [10] have also been advanced to preclinical or clinical trial studies (Fig. 1). Recently, our immense interest in finding effective BTK inhibitors also led to the identification of a set of novel diphenylpyrimidine (DPPY) analogues, including *Pho*-DPPY (**4**) [11], *SFA*-DPPY (**5**) [12] and *Imi*-DPPY (**6**) [13], which exhibited improved anti-B-cell lymphoma activity compared with ibrutinib (Fig. 1). Their structure and activity relationships (SARs) showed that the pyrimidine core, along with a *C*-4 *N*-phenylacrylamide functionality are essential for their high anti-BTK activity. The co-crystal structure of the typical BTK inhibitor **1** with the BTK enzyme also revealed that the acryloyl substituent binds strongly through a covalent bond to the Cys481 residue in the BTK enzyme, while the *C*-2 aniline side chain of the pyrimidine core is in tight contact with the Ser538, Asp539 and Lys430 residues at the bottom of the ATP-binding pocket. All these binding forces contribute to the strong inhibitory potency of this BTK inhibitor [11-16].

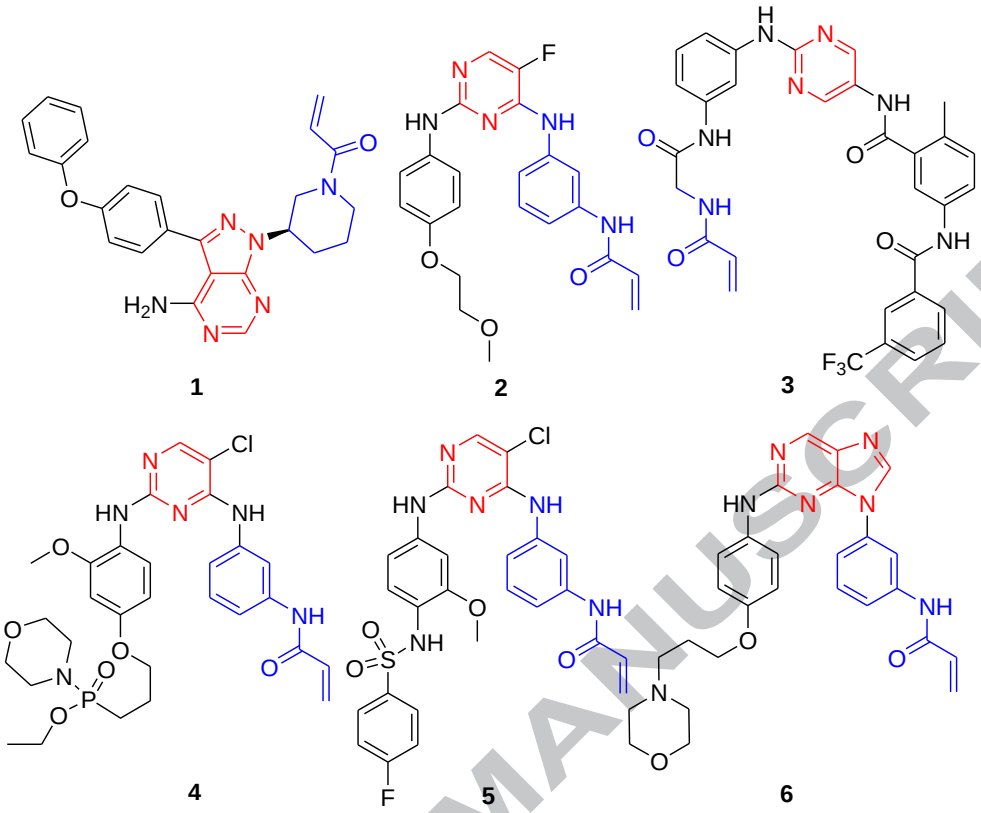

Fig. 1 Structures of the novel BTK inhibitors.

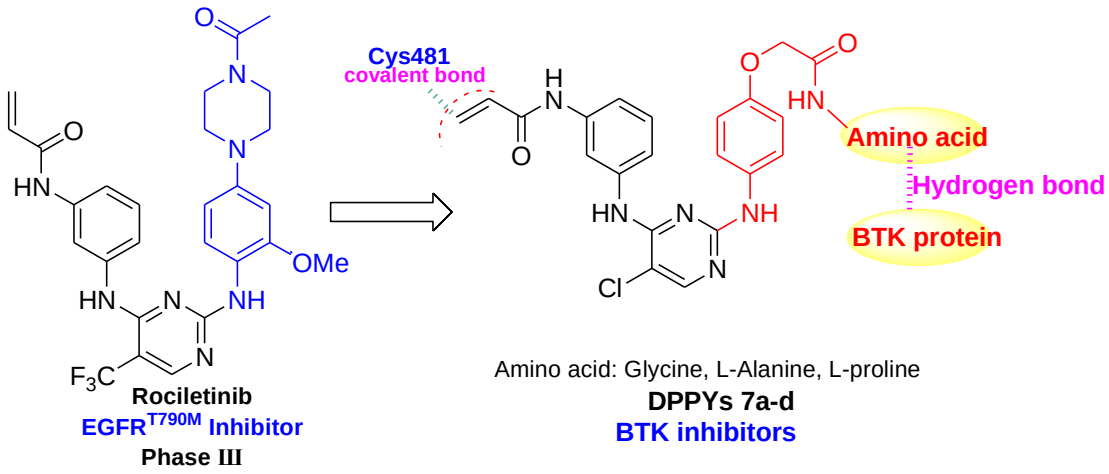

Fig. 2 Discovery strategy of the new DPPYs as potent BTK inhibitors.

Amino acid-substituted derivatives, especially the short synthetic and long-acting peptide, are involved in a variety of physiological and pathological processes. Drugs that bear an amino acid functionality play very important roles in modulating various cell functions, and have been successfully applied to treat certain human diseases [17,18]. For example, goserelin (a synthetic gonadotropin-releasing hormone analog,

marketed as Zoladex®) is applied to treat breast cancer and prostate cancer [19], glatiramer acetate (a synthetic peptide with four amino acids, marketed as Copaxone®) is used to treat multiple sclerosis [20], and exenatide (a synthetic glucagon-like peptide-1 analog, marketed as Byetta®) is used to treat type 2 diabetes [21]. Accordingly, amino acid derivatives do favor forming hydrogen-bonds with proteins, thus contributing to enhance the contact with target proteins [22,23]. Therefore, various amino acid -substituted aniline side chains were installed on the *C*-2 position of the pyrimidine scaffold to form strong hydrogen bond with BTK (Fig. 2). The synthesis of these amino acid-substituted DPPY derivatives, and their biological evaluation of their activity against the BTK enzyme and B-cell lymphoma cell lines are described in this study.

2. Results and Discussion

2.1 Chemistry

The amino acid -substituted pyrimidine analogues were synthesized as illustrated in Scheme 1. 3-Nitroaniline (**8**) was reacted with acryloyl chlorine in the $NaHCO_3$ base to produce the intermediate *N*-acryloyl-4-nitrobenzamide (**9**), which was then reduced by the Fe-NH_4Cl reagent to form the 4-aminobenzamide derivative (**10**). After regioselective substitution of the *C*-4 chlorine atom in the 2,4,5-trichloropyrimidine reagent with aniline **10**, the key pyrimidine intermediate **11** was prepared. Generally, the *C*-2 aniline side chains **12a-d** were conveniently synthesized *via* nucleophilic substitution, dehydration reaction, and reduction reaction according to our previously reported procedures [24,25]. Finally, through the coupling reactions of **11** with aniline intermediates **12a-d** under the action of trifluoroacetic acid (TFA) at reflux temperature, the title molecules **7a-d** were obtained with yield ranging from 12 to 23% [26].

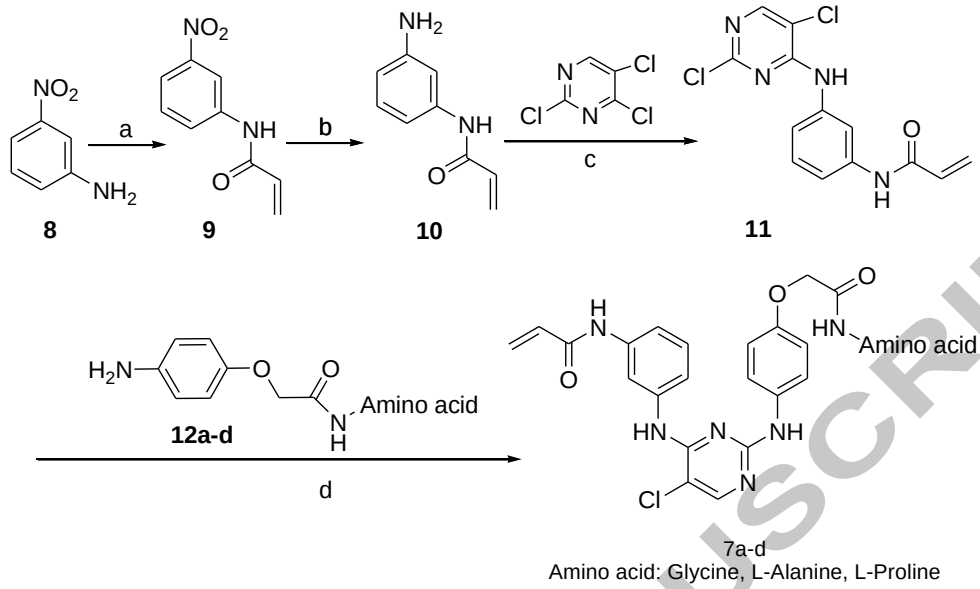

Scheme 1. Synthetic route of title compounds **7a-d**. Reagents and conditions: (a) acryloyl chloride, $NaHCO_3$, CH_3CN, rt, 0.5 h, 95%; (b) Fe-NH_4Cl, MeOH-H_2O, 2 h, 70 °C, 72%; (c) 2,4,5-trichloropyrimidine, DIPEA, *i*-PrOH, 60°C, 2 h, 83%; (d) trifluoroacetic acid, intermediates **12a-d**, 2-BuOH, 100 °C, 12 h, 12% to 23%.

Table 1. Biological activity of theamino acid -substituted diphenylpyrimidine derivatives **7a-d**.

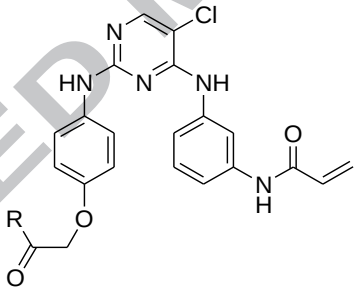

Compd.	R	Enzymatic activity (IC_{50}, nM)		Cellular antiproliferative activity (IC_{50}, μM)[a]		
		JAK3	BTK	NAMALWA	Ramos	Raji
7a	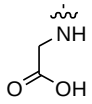	>500.0	11.2	>40.0	>40.0	>40.0
7b	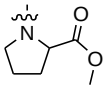	196.0	8.7	4.8±1.1	19.7±3.2	6.7±1.2
7c	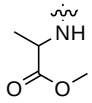	>500.0	8.7	29.3±2.6	40.8	25.2±1.5
7d	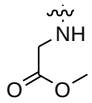	496.0	6.5	16.9±3.1	20.9±3.3	18.0±2.1

Ibrutinib	<100.0	0.4	19.6	5.14	19.5

[a] Data represent the mean of at least three separate experiments. Dose-response curves were determined at five concentrations. The IC_{50} values are the concentrations in nano- or micro-molar needed to inhibit cell growth by 50%, as calculated using GraphPad Prism version 5.0.

2.2 Biological activity

All theamino acid-substitute pyrimidine analogues were evaluated for their potency to inhibit the phosphorylation of BTK, EGFRT790M and the JAK3 enzymes using the ADP-Glo^{TM} kinase assay system (Promega, USA) [27,28]. Moreover, their antiproliferative activity against the B-cell lymphoma cell lines (Raji, Ramos, NAMALWA) were also evaluated with the CCK-8 assay [29]. For comparison, the representative anti-BTK agent ibrutinib was evaluated as well. The results of the biological evaluations are presented in Table 1. These results showed that most of these compounds effectively inhibited the BTK enzymatic activity at concentrations ranging from 6.5 to 11.2 nM. Interestingly, these molecules are not active against both EGFRT790M and the JAK3 enzymes (IC_{50} >100 nM), indicating their improved selectivity against BTK kinase. According to the kinase-based test result, it clearly can be seen that the ester derivatives, including the L-alanine methyl ester, L-proline methyl ester, and glycine methyl ester, which was installed on the *C*-2 aniline side chain is favorable. Nevertheless, the acid derivative **7a**, which was obtained by hydrolyzing the ester substituent in compound **7d**, has slightly reduced anti-BTK enzymatic activity. In addition, their activity against the B-cell lymphoma cells also showed that theseamino acid -substituted molecules could significantly inhibited the proliferation of B-cell lymphoma cells at concentrations in the range of 4.8 to 29.3 μM. Apparently, the molecule **7a** bearing an L-alanine amino acid is less effective in inhibiting B-cell lymphoma cells, with an IC_{50} value higher than 40 μM. Notably, the L-proline-substituted pyrimidine **7b** displayed remarkably improved anti-proliferative activity against NAMALWA (IC_{50} = 4.8 μM) and Raji (IC_{50} = 6.7 μM) cells compared with ibrutinib. Although L-alanine-substituted compound **7d** and glycine-substituted compound **7c** are as potent as L-proline-substituted **7b** in inhibiting the BTK enzymatic activity, both of them are less active against the B-cell

lymphoma cell lines (NAMALWA, Ramos and Raji). Possibly, the slightly high hydrophilicity of the tetrahydropyrrole substituent in compound **7b** results in its enhanced anti-cancer activity. Compared with the novel drug ibrutinib, compound **7b** also displayed approximately 4 times higher activity to interfere with the proliferation of NAMALWA cells, and 3-times higher activity to inhibit Raji cells activity, respectively. Owing to these excellent kinase- and cell-based biological property, compound **7b** was selected to perform the further biological evaluation. The 4',6-diamidino-2-phenylindole (DAPI) and AO/ EB staining assays for the potent inhibitor **7b** showed its higher pro-apoptotic activity in NAMALWA cells than that of ibrutinib at similar concentration (5 μM) (Fig. 3). Furthermore, the effects of compound **7b** were also analyzed in normal peripheral blood mononuclear cells (PBMC) using the AO/EB staining assay. The results of the analysis revealed its low cytotoxicity at concentrations of 5, 10 and 20 μM (Fig. 4). Additionally, inhibitor **7b** also exerted significant effects on the viability of NAMALWA cells in a dose- and time-dependent manner. Also, treatment with inhibitor **7b** at the concentration of 2 μM for 72 h almost completely inhibited NAMALWA cells (Fig. 5).

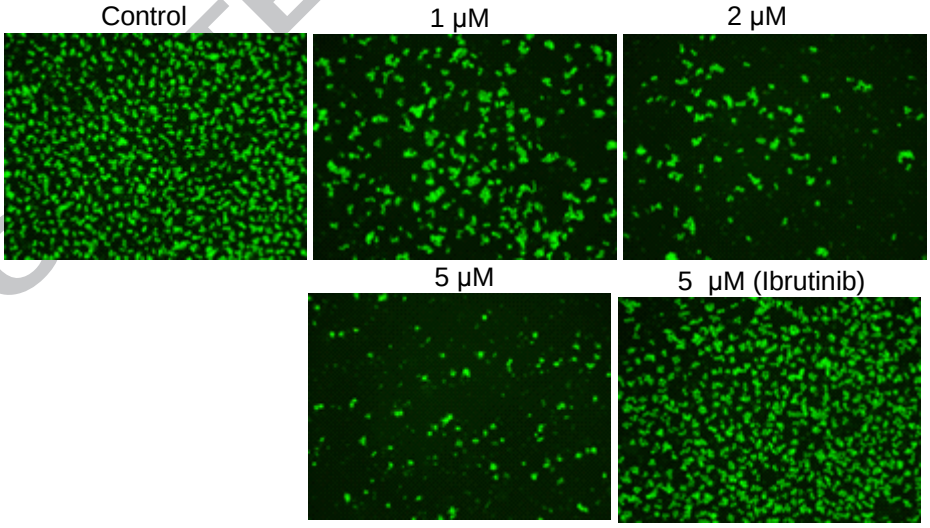

Fig. 3 AO/EB staining assays for the potent compound **7b**.

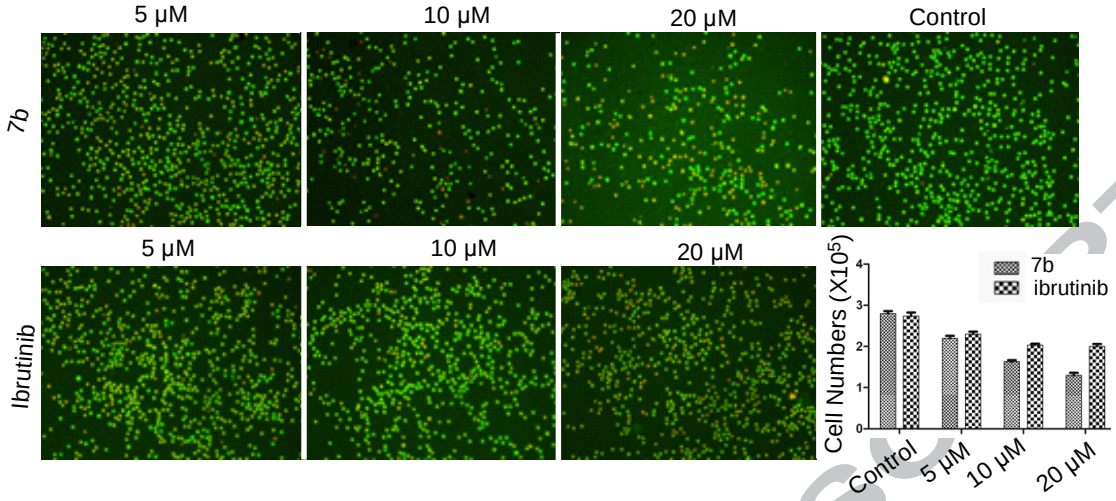

Fig. 4 Cell cytotoxicity of compound **7b** against the normal PBMC cells.

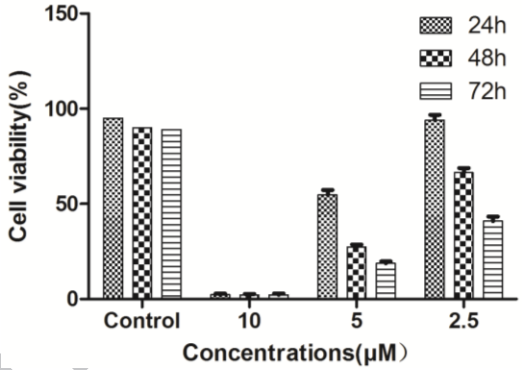

Fig. 5 The effects of compound **7b** on the cell viability of NAMALWA cells.

Apoptosis is a biologically important type of cell death. The effect of compound 7b, the most active BTK inhibitor, on apoptosis was evaluated by flow cytometry analysis of NAMALWA cells incubated with 1, 2 and 5 μM of compound **7b** for 48 h. The analysis results shown in Fig. 6, revealled that inhibitor 7b induced apoptosis in NAMALWA cells, increasing the apoptosis rate from 10.77 to 22.08%. Noteworthy, even at a low concentration of 1 μM, compound 7b induced higher apoptosis rate (140.77%) than the reference agent ibrutinib (9.81%) at a concentration of 5 μM.

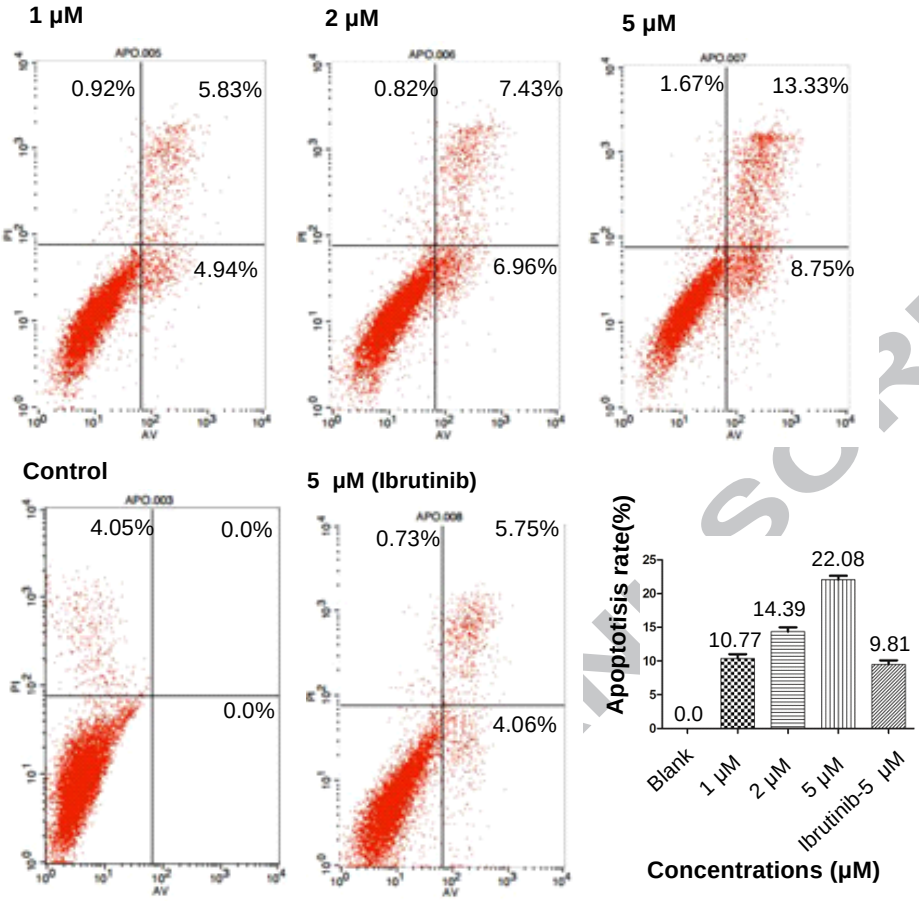

Fig. 6 Compound **7b** induced NAMALWA cell apoptosis *in vitro*. The cells were incubated with the indicated concentrations of **7b** for 48 h, and the cells were stained with annexin V/FTIC, followed by flow cytometry analysis. One representative experiment is shown. $p < 0.05$.

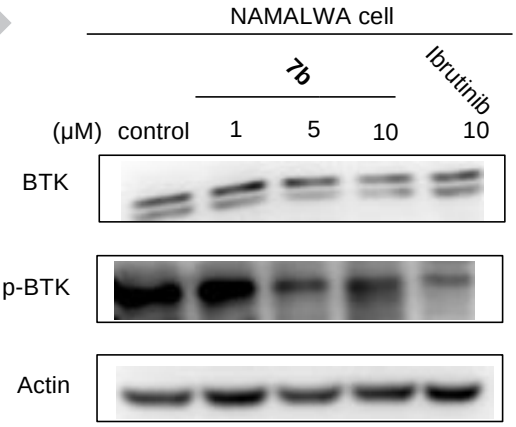

Fig. 7 Compound **7b** and ibrutinib inhibited the activation of EGFR and downstream signaling in NAMALWA cells harboring BTK protein.

To evaluate the effects of theamino acid-substituted pyrimidine derivatives on the BTK activation and downstream signaling, the most active inhibitor **7b** was tested for its capability to interfere with the BTK activation and downstream signaling in NAMALWA cells using ibrutinib as a control. The cells were treated with various

concentrations (1, 5, 10 µM) of inhibitor **7b** for 48 h, and the expression and activation of BTK and phosphorylated BTK (p-BTK) were determined by immunoblotting analysis. The Western blot analysis results, presented in Fig. 7, clearly showed that treatment with **7b** inhibited the phosphorylation of BTK in a dose-dependent manner. Additionally, compound **7b** displayed as strong inhibitory activity as that of ibrutinib, at the same drug concentration (10 µM).

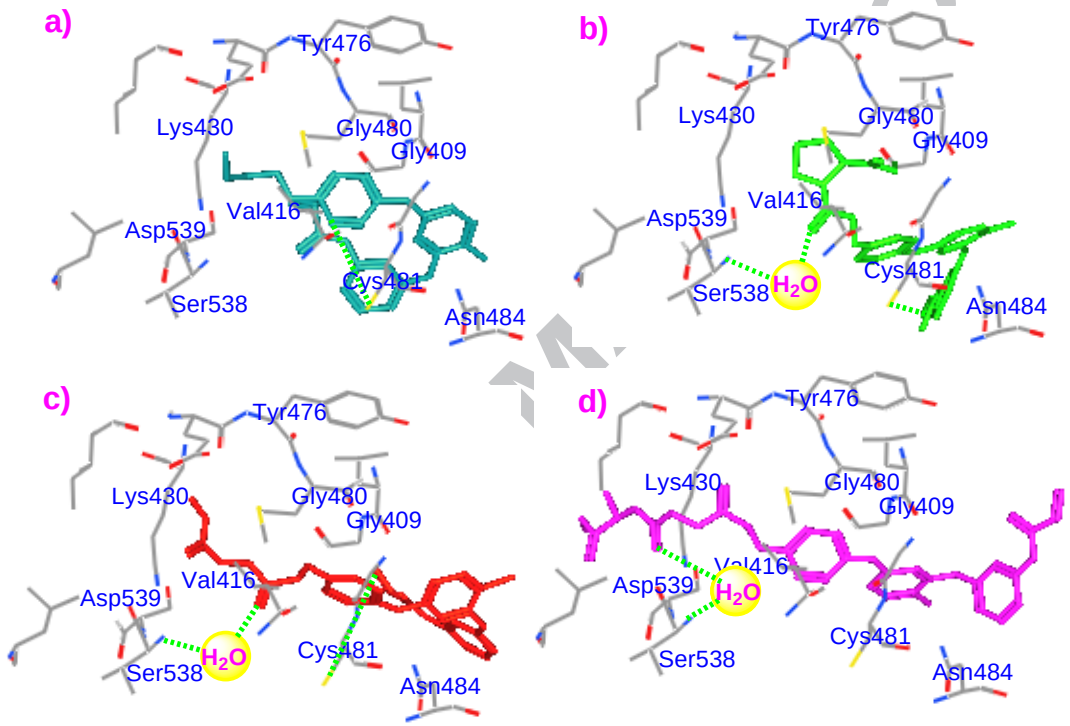

Fig. 8 Putative binding models of spebrutinib and the title molecules within BTK enzyme (PDB code: 3GEN), a): spebrutinib, b): inhibitor **7b**, c): inhibitor **7d**, d): inhibitor **7a**.

2.3 Molecular docking

Using computer molecular simulation technology, we also examined the putative binding mechanism of theamino acid-substituted analogues with the BTK protein. Two of the most active inhibitors, namely **7b** and **7d**, in parallel with a less potent inhibitor, namely **7a,** were separately docked into the binding pocket of the BTK protein (PDB code: 3GEN) [30]. The optimal binding conformations were obtained, using the Autodock 4.2 software and its default parameters [31,32], and are presented in Figures 8a-d. As expected, the designed pyrimidine derivatives form a strong

hydrogen bond between the introducedamino acid functionality with the amino acid Ser538 *via* a water molecule. However, for spebrutinib, this binding force is not present. Moreover, although the two potent inhibitors **7b** and **7d** formed the important covalent bond with the Cys481 residue as spebrutinib, the pyrimidine core in **7b** and **7d** moved farther away from the binding pocket than that in spebrutinib, thus resulting in a significantly reduced anti-BTK activity (approximately 10 times lower). For the less active inhibitor **7a**, this movement also caused the loss of the important covalent bond between acryoylamide with the Cys481 residue. Accordingly, compound **7a** has approximately 11-fold lower anti-BTK activity than compound **7b.** In a word, these binding modes exactly explain the anti-BTK activity data.

3. Conclusion

A class of diphenylpyrimidine derivatives bearing aamino acid functionality were synthesized and biologically evaluated their biological activity against BTK kinase. Notably, compound **7b**, the most active inhibitor in this set of molecules, displayed strong activity against BTK, with an IC_{50} of 8.7 nM. The cell-based activity assay also showed that **7b** had a similar level of potency to inhibit the proliferation of B-cell lymphoma cells. In addition, its effects on normal PBMC cells showed its low cytotoxicity. Other biological evaluations, including the AO/EB staining assay, Western blot analysis and flow cytometry analysis also suggested the high potency of this compound to block the proliferation of B-cell lymphoma cells. Moreover, the molecular simulation analysis revealed that **7b** was in tight contact with the BTK enzyme by forming additional strong hydrogen bonds. Overall, this study provided a new insight to improve the activity ofamino acid-substituted diphenylpyrimidine derivatives against the BTK enzyme.

4. Experimental section

4.1. General methods for chemistry

All reagents and solvents were obtained from commercial sources and used without further purification. High resolution ESI-MS was performed on an AB Sciex TripleTOF® 4600 LC/MS/MS system. ^{1}H and ^{13}C NMR datas were obtained on a Bruker Avance at 400 and 100 MHz, respectively. Coupling constants

(*J*) are expressed in hertz (Hz). Chemical shifts (δ) of NMR are reported in parts per million (ppm) units relative to internal control (TMS). All reactions were monitored by TLC, using silica gel plates with fluorescence F254 and UV light visualization. Flash chromatography separations were obtained on Silica Gel (300-400 mesh) using dichloromethane/methanol as eluents.

*4.2. General procedure for the synthesis of **7a-d***

Amino acid-substituted anilines **12a-d**, and 2-chloropyrimidine **11**were generally synthesized according to the methods reported by us and others [24-26]. All these intermediates were used without any purification and structural characterization. With these intermediates in hand, the desired compounds were synthesized as described below.

A flask was charged with compounds **11** (1.0 mmol), anilines **12a-d,** (1.0 mmol), TFA (342 mg. 3 mmol), and 2-BuOH (15 mL). The slurry was heated to 100 ℃ for 12 h. The reaction mixture was allowed to cool to room temperature and was neutralized with a saturated aqueous sodium bicarbonate solution. The aqueous mixture was then extracted with CH_2Cl_2 (20 mL) three times. The crude product was purified by using flash chromatography with dichloromethane/methanol (v/v, **12a**: 15/1; **12c-d**: 30/1) as eluents.

4.2.1. N-[3-[[5-Chloro-2-[4-[2-[(carbonylmethyl)amino]-2-oxoethoxy]phenylamino]-4-pyrimidinyl]amino]phenyl]-2-acrylamide (**7a**):

Yield, 12%; off-white solid; ^{1}H NMR (400 MHz, DMSO-d_6): ^{1}H NMR (400 MHz, DMSO) δ 10.93(br, 1H), 10.15(s, 1H), 9.43(br, 1H), 8.45-8.48(m, 1H), 8.22(s, 1H), 7.67(s, 1H), 7.51-7.47(m, 2H), 7.32-7.22(m, 2H), 6.82(d, *J* =8.0 Hz, 2H), 6.77(dd, *J* =16.8, 10.4 Hz, 1H), 6.23(dd, *J* = 16.8, 4.0 Hz, 1H), 5.72(dd, *J* =10.4, 4.0 Hz, 1H), 4.45(s, 2H), 3.83(s, 2H); ^{13}C NMR (100 MHz, DMSO) δ 171.07, 168.41, 168.36, 168.00, 163.49, 156.72, 153.32, 139.59, 139.34, 138.24, 132.22, 128.68, 126.71, 121.68, 121.42 (2C), 114.95 (2C), 114.73, 114.35, 103.93, 67.19, 42.15; HRMS (ESI) *m/z* calcd for $C_{23}H_{21}ClN_6O_5$, $[M+H]^+$ 497.1335, found: 497.1414.

4.2.2. *N*-[3-[[5-Chloro-2-[4-[2-[2-(methoxycarbonyl)-1-pyrrolidinyl]-2-oxoethoxy] phenylamino]-4-pyrimidinyl]amino]phenyl]-2-acrylamide (**7b**): Yield, 22%; off-white solid; ^{1}H NMR (400 MHz, DMSO-d_6): δ10.27(s, 1H), 9.21(s, 1H), 8.88(s, 1H), 8.10(s, 1H), 7.94(s, 1H), 7.51-7.49(m, 3H), 7.34-7.28(m, 2H), 6.71-6.69(d, *J* =8.4 Hz, 2H), 6.50(dd, *J* =16.8, 10.0 Hz, 1H), 6.26(dd, *J* =10.0, 2.0 Hz, 1H), 5.76-5.73(dd, *J* =16.8, 2.0 Hz, 1H), 4.75-4.66(m, 1H), 4.65(s, 2H), 3.62-3.37(m, 2H), 3.37 (s, 3H), 1.94(m, 2H), 1.50(m, 2H); ^{13}C NMR (100 MHz, DMSO) δ 171.82, 166.70, 163.62, 158.24, 156.52, 155.19, 153.21, 139.60, 139.39, 134.41, 132.42, 129.00, 127.31, 120.89(2C), 115.58, 115.40, 114.67, 114.48(2C), 103.85, 72.62, 66.77, 59.36, 45.97, 28.64, 19.64; HRMS (ESI) *m/z* calcd for $C_{27}H_{27}ClN_6O_5$, $[M+H]^+$ 551.1804, found: 551.1886.

4.2.3. (*S*)-*N*-[3-[[5-Chloro-2-[4-[2-[2-(methoxycarbonylethyl)amino]-2-oxoethoxy] phenylamino]-4-pyrimidinyl]amino]phenyl]-2-acrylamide (**7c**): Yield, 18%; off-white solid; ^{1}H NMR (400 MHz, DMSO-d_6): δ 10.22(s, 1H), 9.22(s, 1H), 8.95(s, 1H), 8.49(s, 1H), 8.16(s, 1H), 7.93(s, 1H), 7.56-7.54(m, 3H), 7.37(d, *J* =8.0 Hz, 2H), 6.80(d, *J* =8.0 Hz, 2H), 6.48(dd, *J* =16.8, 12.0 Hz, 1H), 6.33(dd, *J* =16.8, 4.0 Hz, 1H), 6.02-5.79(dd, *J* =12.0, 4.0 Hz, 1H), 4.46-4.42(m, 3H), 3.67(s, 3H), 1.38(d, *J* =8.0 Hz, 3H); ^{13}C NMR (100 MHz, DMSO) δ 172.43, 168.26, 163.61, 158.22, 156.57, 155.22, 152.92, 139.56, 139.37, 134.73, 132.37, 129.00, 127.38, 120.84(2C), 119.56, 115.83, 115.53, 114.91(2C), 103.89, 72.82, 67.54, 48.11, 17.35; HRMS (ESI) *m/z* calcd for $C_{25}H_{25}ClN_6O_3S$, $[M+H]^+$ 525.1648, found: 525.1733.

4.2.4. (*S*)-*N*-[3-[[5-Chloro-2-[4-[2-[(methoxycarbonylmethyl)amino]-2-oxoethoxy] phenylamino]-4-pyrimidinyl]amino]phenyl]-2-acrylamide (**7d**): Yield, 19%; off-white solid; ^{1}H NMR (400 MHz, DMSO) δ 10.26(s, 1H), 9.23(s, 1H), 8.91(s, 1H), 8.47-8.45(d, *J* =8.0 Hz, 1H), 8.12(s, 1H), 7.94(s, 1H), 7.53-7.51(m, 3H), 7.32(d, *J* = 8.0 Hz, 2H), 6.76(d, *J* =8.0 Hz, 2H), 6.52-6.46(dd, *J* =16.0, 12.0 Hz, 1H), 6.28-6.24(*J* =16.0 Hz, 1H), 5.77-5.74(*J* =12.0 Hz, 1H), 4.42(s, 2H), 3.63(s, 3H), 3.37(s, 2H); ^{13}C NMR (100 MHz, DMSO) δ 172.76, 167.81, 163.15, 157.70, 156.10, 154.67, 152.41, 139.09, 138.89, 134.23, 131.90, 128.54, 126.91, 120.39(2C), 119.06, 115.35, 115.02,

114.46(2C), 103.40, 67.04, 51.96, 47.27; HRMS (ESI) *m/z* calcd for $C_{24}H_{23}ClN_6O_5$, $[M+H]^+$ 511.1491, found: 511.1421.

4.3. Kinase enzymatic assays

Enzymatic assays were tested by using the ADP-Glo™ assay system (BTK: Catalog. **V2941**, JAK3: Catalog. **V3701,** Promega). The experiments were performed according to the instructions of the manufacturer. The detailed and complete protocols, and the active kinase data were available at: https://cn.promega.com/products/cell-signaling/kinase-assays-and-kinase-biology/btk-kinase-enzyme-system/?catNum=V2941 and https://cn.promega.com/products/cell-signaling/kinase-assays-and-kinase-biology/jak3-kinase-enzyme-system/?catNum=V3701), respectively. For all of the tested compounds, concentrations consisting of suitable levels from 0.1 to 1000 nM were used. The test was performed in a 384-well plates, including the main steps below: (1) perform a 5 μL kinase reaction using 1× kinase buffer (e.g., 1× reaction buffer A), (2) incubate at room temperature for 60 minutes, (3) add 5 μL of ADP-Glo™ reagent to stop the kinase reaction and deplete theunconsumed ATP, leaving only ADP and a very low background of ATP, (4) incubate at room temperature for 40 minutes, (5) add 10 μL of kinase detection, (6) reagent to convert ADP to ATP andintroduce luciferase and luciferin to detect ATP, (7) incubate at room temperature for 30 minutes, (8) plates was measured on TriStar® LB942 Multimode Microplate Reader (BERTHOLD) to detect the luminescence (Integration time 0.5-1 second). Curve fitting and data presentations were performed using GraphPad Prism version 5.0.

4.4.Cell and reagents

4.4.1.Cellular activity assay

Ramos, Raji and NAMALWA cells were purchased from Fuheng Biology Company (Shanghai, China). Cell viability assays were performed by using CCK-8 reagent (Biotool Company). The cells were seeded in 96-well plates at a density of 3,000 cells/well and were maintained at 37 °C in a 5% CO_2 incubator in RPMI-1640 containing 10% fetal bovine serum (FBS, Gibco) for 4 h. Cells were exposed to

treatment for 72 h, and the number of cells used per experiment for each cell lines was adjusted to obtain an absorbance of 0.5 to 1.2 at 450 nm with a microplate reader (Thermo Fisher, USA). Compounds were tested at appropriate concentrations (1.25 to 40 μM), with each concentration duplicated five times. The IC_{50} values were calculated using GraphPad Prism version 5.0.

4.4.2.Cytotoxic activity assay

Peripheral venous blood was collected in an ACD anticoagulant (V_{blood}: $V_{anticoagulant}$ = 9:1) tube from the normal healthy adult male. The leucocyte-rich plasma was removed and the peripheral blood mononuclear cells (PBMC) consisting of monocytes and the lymphocytes were separated on Lymphoprep (density 1.077g/ml, Nyegaard & Co. As., Oslo, Norway). The cells collected from the interface layer were washed three times with PBS buffered salt solution and counted using cell counting chamber.

PBMC cells were seeded in 24-well plates at a density of 200,000 to 250,000 cells/well. Cells were treated with inhibitors **7b** and Ibrutinib at appropriate concentrations (1, 2, 5 μM), with each concentration duplicated five times. Aftering maintaining the cells at 37 °C in a 5% CO_2 incubator in RPMI-1640 containing 10% fetal bovine serum (FBS, Gibco) for 24 h, the morphology of the cells was observed with a phase contrast microscope (Nikon, Japan), and the number of living PBMC cells was calculated by traditional manual method with an ordinary cell counting chamber.

4.5.Flow cytometry assay

The NAMALWA cells (1×10^6 cells/well) incubated in 6-well plates were treated with solvent control (DMSO), ibrutinib, or compounds **7b** in medium containing 5% FBS for 72 h. Then, collected and fixed with 70% ethanol at 4 ℃ overnight. After being fixed with 70% ethanol at 4 °C, the cells were stained with Annexin V-FITC (5 μL)/propidium iodide (5 μL), and analyzed by flow cytometry assay (Becton-Dickinson, USA).

4.6.Western blotting assay

The lysates from Namalwa cells in different groups were extracted and centrifuged at 14,000 g for 15 min at 4 °C, then the total proteins were obtained. An aliquot (50 μg protein) was loaded onto a 8%-12% SDS-PAGE gels and separated electrophoretically. Then the target proteins were transferred to a PVDF membrane (Millipore, USA). After blocking the PVDF membrane in 5% dried skim milk (Boster Biological Technology, China) for 2 h at room temperature, the membrane was incubated overnight at 4 °C with primary antibodies for 12 h. Protein detection was performed based on an enhanced chemiluminescence (ECL) method and photographed by using a BioSpectrum Gel Imaging System (HR410, UVP, USA). In order to eliminate the variations, data were adjusted to β-Actin expression: IOD of objective protein versus IOD of β-Actin expression.

4.7. Molecular docking study

Docking studies were carried out on AutoDock 4.2. The crystal structure (PDB: 3GEN) of the kinase domain of BTK bound to a pyrrolopyrimidine-containing compound. The enzyme preparation and the hydrogen atoms adding was performed in the prepared process. The whole BTK enzyme was defined as a receptor and the site sphere was selected on the basis of the binding location of pyrrolopyrimidine inhibitor. By moving the inhibitor and the irrelevant water, molecules **7a, b**, **7d** were placed, respectively.The binding interaction energy was calculated to include van der Waals, electrostatic, and torsional energy terms defined in the tripos force field. Ten docking poses were generated and clustered, and compounds with predicted binding affinities better than) 7.0 kcal⁄mol in each of the three docking runs were selected for further analysis and visual inspection. During the performance, the covalent bond between the acrylamide group and the amino acid Cys481 was set as default when the distance beween them lower than 2.82 Å (spebrutinib could form covalent bond in this distance). The structure optimization was performed using a genetic algorithm, and only the best-scoring ligand protein complexes were kept for analyses.

Acknowledgements

We are grateful to the National Natural Science Foundation of China (No. 81672945, 81603186), and the Research Fund of Higher Education of liaoning province (No. LF2017008, LQ2017039) for the financial support of this research.

References

[1] Küppers R. Mechanisms of B-cell lymphoma pathogenesis. Nat Rev Cancer. 2005; 5: 251−62.

[2] Seiler T, Dreyling M. Bruton's tyrosine kinase inhibitors in B-cell lymphoma: current experience and future perspectives. Expert Opin Investig Drugs. 2017; 26: 909−15.

[3] Adem J, Eray M, Eeva J, Nuutinen U, Pelkonen J. Advantages of targeting B cell receptor complex to treat B-cell derived autoimmune diseases and lymphomas. Mol Immunol. 2017; 88: 135−7.

[4] Corneth OB, Klein Wolterink RG, Hendriks RW. BTK signaling in B cell differentiation and autoimmunity. Curr Top Microbiol Immunol. 2016; 393: 67−105.

[5] Robak P, Robak T. Novel synthetic drugs currently in clinical development for chronic lymphocytic leukemia. Expert Opin Investig Drugs. 2017; 26: 1−17.

[6] Honigberg LA, Smith AM, Sirisawad M, Verner E, Loury D, Chang B, Li S, Pan Z, Thamm DH, Miller RA, Buggy JJ. The Bruton tyrosine kinase inhibitor PCI-32765 blocks B-cell activation and is efficacious in models of autoimmune disease and B-cell malignancy. Proc Natl Acad Sci U S A. 2010; 107: 13075−80.

[7] de Rooij MF, Kuil A, Geest CR, Eldering E, Chang BY, Buggy JJ, Pals ST, Spaargaren M. The clinically active BTK inhibitor PCI-32765 targets B-cell receptor- and chemokine-controlled adhesion and migration in chronic lymphocytic leukemia. Blood. 2012; 119: 2590−4.

[8] de Claro RA, McGinn KM, Verdun N, Lee SL, Chiu HJ, Saber H, Brower ME, George Chang CJ, Pfuma E, Habtemariam B, Bullock J, Wang Y, Nie L, Chen XH, Lu DR, Al-Hakim A, Kane RC, Kaminskas E, Justice R, Farrell AT, Pazdur R. FDA Approval: Ibrutinib for patients with previously treated mantle cell lymphoma and previously treated chronic lymphocytic leukemia. Clin Cancer Res. 2015; 21: 3586−90.

[9] Evans E, Ponader S, Karp R,Tester R, Sheets M, Aslanian S, Martin, TS, Nacht M, Zhu Z, Chaturvedi P, Witowski S, Lounsbury H, Stiede K, Burger J, Petter R,

Singh J, Westlin WF. Covalent inhibition of Btk with clinical development compound AVL-292 disrupts signaling that maintains the microenvironment necessary for chronic lymphocytic leukemia growth. Cl Lymph Myelom Leuk. 2011; 11: S173−4.

[10] Li X, Zuo Y, Tang G, Wang Y, Zhou Y, Wang X, Guo T, Xia M, Ding N, Pan Z. Discovery of a series of 2,5-diaminopyrimidine covalent irreversible inhibitors of Bruton's tyrosine kinase with *in vivo* antitumor activity. J Med Chem. 2014; 57: 5112−28.

[11] Ge Y, Yang H, Wang C, Meng Q, Li L, Sun H, Zhen Y, Liu K, Li Y, Ma X. Design and synthesis of phosphoryl-substituted diphenylpyrimidines (*Pho*-DPPYs) as potent Bruton's tyrosine kinase (BTK) inhibitors: Targeted treatment of B lymphoblastic leukemia cell lines. Bioorg Med Chem. 2017; 25: 765−72.

[12] Liu H, Qu M, Xu L, Han X, Wang C, Shu X, Yao J, Liu K, Peng J, Li Y, Ma X. Design and synthesis of sulfonamide-substituted diphenylpyrimidines (*SFA*-DPPYs) as potent Bruton's tyrosine kinase (BTK) inhibitors with improved activity toward B-cell lymphoblastic leukemia. Eur J Med Chem. 2017; 135: 60−9.

[13] Ge Y, Jin Y, Wang C, Zhang J, Tang Z, Peng J, Liu K, Li Y, Zhou Y, Ma X. Discovery of novel Bruton's tyrosine kinase (BTK) inhibitors bearing a *N*,9-diphenyl-9*H*-purin-2-amine scaffold. ACS Med Chem Lett. 2016; 7: 1050−5.

[14] Seiler T, Dreyling M. Bruton's tyrosine kinase inhibitors in B-cell lymphoma: current experience and future perspectives. Expert Opin Investig Drugs. 2017; 26: 909−15.

[15] Zhao D, Huang S, Qu M, Wang C, Liu Z, Li Z, Peng J, Liu K, Li Y, Ma X, Shu X. Structural optimization of diphenylpyrimidine derivatives (DPPYs) as potent Bruton's tyrosine kinase (BTK) inhibitors with improved activity toward B leukemia cell lines. Eur J Med Chem. 2017; 126: 444−55.

[16] Wang B, Deng Y, Chen Y, Yu K, Wang A, Liang Q, Wang W, Chen C, Wu H, Hu C, Miao W, Hur W, Wang W, Hu Z, Weisberg EL, Wang J, Ren T, Wang Y, Gray NS, Liu Q, Liu J. Structure-activity relationship investigation for benzonaphthyridinone derivatives as novel potent Bruton's tyrosine kinase (BTK) irreversible inhibitors. Eur J Med Chem. 2017; 137: 545−57.

[17] Kukowska M. Amino acid oramino acid conjugates of acridine/acridone and quinoline/quinolone-containing drugs. A critical examination of their clinical

effectiveness within a twenty-year timeframe in antitumor chemotherapy and treatment of infectious diseases. Eur J Pharm Sci. 2017; 109: 587−615.

[18] Chen SW, Van Regenmortel MH, Pellequer JL. Structure-activity relationships in peptide-antibody complexes: implications for epitope prediction and development of synthetic peptide vaccines. Curr Med Chem. 2009; 16: 953−64.

[19] Saphner T, Troxel AB, Tormey DC, Neuberg D, Robert NJ, Pandya KJ, Edmonson JH, Rosenbluth RJ, Abeloff MD. Phase II study of goserelin for patients with postmenopausal metastatic breast cancer. J Clin Oncol. 1993; 11: 1529−35.

[20] Bell C, Anderson J, Ganguly T, Prescott J, Capila I, Lansing JC, Sachleben R, Iyer M, Fier I, Roach J, Storey K, Miller P, Hall S, Kantor D, Greenberg BM, Nair K, Glajch J. Development of Glatopa® (Glatiramer Acetate): The first FDA-Approved generic disease-modifying therapy for relapsing forms of multiple sclerosis. J Pharm Pract. 2017; doi: 10.1177/0897190017725984.

[21] DeFronzo RA, Okerson T, Viswanathan P, Guan X, Holcombe JH, MacConell L. Effects of exenatide versus sitagliptin on postprandial glucose, insulin and glucagon secretion, gastric emptying, and caloric intake: a randomized, cross-over study. Curr Med Res Opin. 2008; 24: 2943−52.

[22] Ludwig R, Khudozhitkov AE, Stange P, Golub B, Paschek D, Stepanov AG, Kolokolov DI. Characterization of doubly ionic hydrogen bonds in protic ionic liquids by NMR deuteron quadrupole coupling constants: differences to H-bonds in amides, peptides, and proteins. Angew Chem Int Ed Engl. 2017; 56: 14310−4.

[23] Qing G, Lu Q, Li X, Liu J, Ye M, Liang X, Sun T. Hydrogen bond based smart polymer for highly selective and tunable capture of multiply phosphorylated peptides. Nat Commun. 2017; 8: 461.

[24] Song Z, Huang S, Yu H, Jiang Y, Wang C, Meng Q, Shu X, Sun H, Liu K, Li Y, Ma X. Synthesis and biological evaluation of morpholine-substituted diphenylpyrimidine derivatives (Mor-DPPYs) as potent EGFR T790M inhibitors with improved activity toward the gefitinib-resistant non-small cell lung cancers (NSCLC). Eur J Med Chem. 2017; 133: 329−39.

[25] Lu C, Kim BM, Lee D, Lee MH, Kim JH, Pyo HB, Chai KY. Synthesis of lipoic acid-peptide conjugates and their effect on collagen and melanogenesis. Eur J Med Chem. 2013; 69: 449−54.

[26] Ge Y, Wang C, Song S, Huang J, Liu Z, Li Y, Meng Q, Zhang J, Yao J , Liu

K, Ma X, Sun X. Identification of highly potent BTK and JAK3 dual inhibitors with improved activity for the treatment of B-cell lymphoma. Eur J Med Chem. 2017, 143;1847-57.

[27] Goueli S, Hsiao K, Vidugiris G, Hennek J, Zegzouti H. ADP-Glo^{TM}: A one platform ideal for assay development, screening and profiling of all phosphotransferases. FASEB J. 2015; 29: 934.1.

[28] Zegzouti H, Zdanovskaia M, Hsiao K, Goueli SA. ADP-Glo: A bioluminescent and homogeneous ADP monitoring assay for kinases. Assay Drug Dev Technol. 2009; 7: 560−72.

[29] Wu H, Wang W, Liu F, Weisberg EL, Tian B, Chen Y, Li B, Wang A, Wang B, Zhao Z, McMillin DW, Hu C, Li H, Wang J, Liang Y, Buhrlage SJ, Liang J, Liu J, Yang G, Brown JR, Treon SP, Mitsiades CS, Griffin JD, Liu Q, Gray NS, Discovery of a potent, covalent BTK inhibitor for B-cell lymphoma, ACS Chem Biol. 2014; 9: 1086−91.

[30] Marcotte DJ, Liu YT, Arduini RM, Hession CA, Miatkowski K, Wildes CP, Cullen PF, Hong V, Hopkins BT, Mertsching E, Jenkins TJ, Romanowski MJ, Baker DP, Silvian LF. Structures of human Bruton's tyrosine kinase in active and inactive conformations suggest a mechanism of activation for TEC family kinases. Protein Sci. 2010; 19: 429−439.

[31] Wildman SA, Zheng X, Sept D, Auletta JT, Rosenberry TL, Marshall GR. Drug-like leads for steric discrimination between substrate and inhibitors of human acetylcholinesterase. Chem Biol Drug Des. 2011; 78: 495−504.

[32] Goodsell DS, Morris GM, Olson AJ. Automated docking of flexible ligands: applications of AutoDock. J Mol Recognit. 1996; 9: 1−5.

Highlights

- New diphenylpyrimidine derivative as potent BTK inhibitors.
- Compound **7b** displayed similar activity against B-cell lymphoma cell lines as ibrutinib.
- Compound **7b** exhibited low cytotoxic activity against normal PBMC cells.
- Western blot analysis and flow cytometry analysis also showed its effectiveness in interfering with B-cell lymphoma cell growth.

Graphic abstract